Anal. Chem. **2002,** *74,* 5754−5765

Extrathermodynamic Relationships in Reversed-Phase Liquid Chromatography

Kanji Miyabe[†] and Georges Guiochon*[,‡]

Faculty of Education, Toyama University, 3190, Gofuku, Toyama 930-8555, Japan, Department of Chemistry, The University of Tennessee, Knoxville, Tennessee 37996-1600, and Division of Chemical and Analytical Sciences, Oak Ridge National Laboratory, Oak Ridge, Tennessee 37831

Enthalpy−entropy compensation (EEC) and linear free energy relationships (LFER) are extrathermodynamic correlations frequently used to discuss the mechanistic similarities of chemical equilibria and reaction kinetics. Although empirical, they are widely applied, proving the substantial effectiveness of fundamental studies based on them. Many attempts have been made to interpret theoretically the necessary conditions (or preconditions) of EEC and LFER. LFER is known to rest on the existence of EEC. However, the intimate correlations between EEC on one hand and LFER and the temperature dependence of LFER on the other hand were insufficiently discussed from the viewpoint of molecular structure contributions. We present a simple LFER model relating the slope and intercept of LFER to the compensation temperatures, themselves derived from EEC analyses, and to several parameters characterizing the molecular contributions to the changes in enthalpy and entropy associated with the passage from one phase of the chromatographic system to the other. A theoretical explanation is supplied for the intimate correlation between the two types of extrathermodynamic relationships, EEC and LFER. We demonstrate also that the characteristics of EEC and LFER depend on the structural parameters. This new model allows a proper interpretation of the temperature dependence of LFER. It should permit further progress of fundamental studies of chemical reaction mechanisms based on extrathermodynamic relationships.

Liquid chromatography (LC) is a powerful and reliable separation technique that is widely used for both analytical and preparative purposes.[1] Among its possible implementations, reversed-phase LC (RPLC) is the most suitable for fundamental studies of the characteristics and strength of intermolecular interactions in liquid−solid adsorption and in other separation mechanisms and for studies of the related mass-transfer kinetics because adsorbates, adsorbents, and solvents can be chosen among a multitude of compounds having a wide range of properties.[1−3] These studies are best carried out using the peak moments that are simply related to the characteristics of retention and equilibration kinetics.[4−8] A most important tool for the investigation of retention mechanisms from the point of view of thermodynamics is the use of enthalpy−entropy compensations (EEC).[9−24] EECs have also been used in a few studies of mass-transfer processes such as surface diffusion.[8,17,25,26] Linear free energy relationships (LFER) constitute another type of useful extrathermodynamic relationships, abundantly used in investigations of retention mechanisms and of mass-transfer kinetics.[8] This work is concerned with the new use of LFER involving both retention equilibria and mass-transfer kinetics, an area in which there has been so far no theoretical work. This investigation has lead us to an analysis of the fundamental background relating EEC and LFER.

Chromatographic separations are based on the differences in the free energy changes (ΔG) associated with the adsorption of

* Corresponding author. E-mail: guiochon@utk.edu.
[†] Toyama University.
[‡] University of Tennessee and Oak Ridge National Laboratory.

(1) Guiochon, G.; Golshan-Shirazi, S.; Katti, A. M. *Fundamentals of Preparative and Nonlinear Chromatography*; Academic Press: Boston, 1994.
(2) Giddings, J. C. *Dynamics of Chromatography, Part I, Principles and Theory*; Marcel Dekker: New York, 1965.
(3) Carr, P. W., Martire, D. E., Snyder, L. R., Eds. *J. Chromatogr., A* **1993**, *656*, 1−615.
(4) Ruthven, D. M. *Principles of Adsorption & Adsorption Processes*; John Wiley and Sons: New York, 1984.
(5) Suzuki, M. *Adsorption Engineering*; Kodansha/Elsevier: Tokyo, 1990.
(6) Reid, R. C.; Prausnitz, J. M.; Sherwood, T. K. *The Properties of Gases and Liquids*; McGraw-Hill: New York, 1977.
(7) Miyabe, K.; Guiochon, G. *Anal. Chem.* **2000**, *72*, 5162−5171.
(8) Miyabe, K.; Guiochon, G. *Adv. Chromatogr.* **2000**, *40*, 1−113.
(9) Leffler, J. E.; Grunwald, E. *Rates and Equilibria of Organic Reactions*; Wiley: New York, 1963.
(10) Hammett, L. P. *Physical Organic Chemistry*; McGraw-Hill: New York, 1970.
(11) Exner, O. *Nature* **1964**, *201*, 488−490.
(12) Exner, O. *Prog. Phys. Org. Chem.* **1973**, *10*, 411−482.
(13) Exner, O. *Prog. Phys. Org. Chem.* **1990**, *18*, 129−161.
(14) Colin, H.; Diez-Masa, J. C.; Guiochon, G.; Czajkowska, T.; Miedziak, I. *J. Chromatogr.* **1978**, *167*, 41−65.
(15) Melander, W. R.; Campbell, D. E.; Horváth, C. *J. Chromatogr.* **1978**, *158*, 215−225.
(16) Melander, W. R.; Chen, B. K.; Horváth, C. *J. Chromatogr.* **1979**, *185*, 99−109.
(17) Miyabe, K.; Guiochon, G. *J. Phys. Chem. B* **1999**, *103*, 11086−11097.
(18) Miyabe, K.; Guiochon, G. *Anal. Chem.* **1999**, *71*, 889−896.
(19) Krug, R. R.; Hunter, W. G.; Grieger, R. A. *Nature* **1976**, *261*, 566−567.
(20) Krug, R. R.; Hunter, W. G.; Grieger, R. A. *J. Phys. Chem.* **1976**, *80*, 2335−2341.
(21) Krug, R. R.; Hunter, W. G.; Grieger, R. A. *J. Phys. Chem.* **1976**, *80*, 2341−2351.
(22) Krug, R. R. *Ind. Eng. Chem. Fundam.* **1980**, *19*, 50−59.
(23) Boots, H. M. J.; de Bokx, P. K. *J. Phys. Chem.* **1989**, *93*, 8240−8243.
(24) Vailaya, A.; Horváth, C. *J. Phys. Chem.* **1996**, *100*, 2447−2455.
(25) Miyabe, K.; Guiochon, G. *Anal. Chem.* **2000**, *72*, 1475−1489.
(26) Miyabe, K.; Guiochon, G. *J. Chromatogr., A* **2000**, *903*, 1−12.

10.1021/ac020245p CCC: $22.00
Published on Web 10/10/2002

the sample compounds from the mobile onto the stationary phase. Moment analysis of elution peaks based on the general kinetic model provides useful information on the retention equilibrium and the mass-transfer kinetics in the column. This analysis shows that, under linear conditions, the peak first moment, which characterizes its position, depends only on the thermodynamics equilibrium constant (K). Numerous studies of separation mechanisms in LC and of molecular interactions in liquid−solid adsorption systems were made using retention equilibrium parameters because of the high precision of the retention data and the ease of acquisition of these data.[3]

Moment analysis shows also that the peak width is related to several kinetic parameters.[1,4,5] Peak broadening is influenced by the mass-transfer kinetics. The second central moment is the sum of contributions due to the different mass-transfer processes in the column, axial dispersion, the fluid-to-particle mass-transfer, intraparticle diffusion, and the adsorption/desorption kinetics. Furthermore, it is usually assumed that intraparticle diffusion consists of two processes, pore diffusion and surface diffusion.[4,5] The mass-transfer processes listed above could be classified into two groups: (1) the diffusive transport of sample molecules with no influence of the stationary phase, i.e., of the surface of the particles of packing material (e.g., axial dispersion, fluid-to-particle mass transfer, and pore diffusion); and (2) the diffusive transport taking place under the influence of adsorptive interactions (surface diffusion) and adsorption/desorption kinetics. Many fundamental studies have been made on mass-transfer kinetics with no adsorptive interaction because these processes are inherent to all flow operations using fixed beds packed with porous materials. Much information is available on the characteristic features of axial dispersion, fluid-to-particle mass transfer, and pore diffusion. Various literature correlations have also been proposed to estimate the related diffusivities and mass-transfer coefficients.[1,4−6]

By contrast, there are still many poorly understood issues involved in surface diffusion and the adsorption/desorption kinetics, their intrinsic characteristics, and their mechanisms. These features depend on intermolecular interactions between the sample compound and the stationary phase. It is usually assumed that the actual adsorption/desorption rate is fast enough in RPLC so that its contribution to the overall mass-transfer resistance in the column is negligibly small.[7] By contrast, surface diffusion plays an important role in intraparticle diffusion.[8] Because surface diffusion is a form of molecular migration in the adsorbed state, it is affected by the adsorptivity of the sample compound, quantitatively accounted for by the equilibrium constant, K. Because chromatographic separations are based on the differences between the adsorptive interactions of the different sample compounds with the stationary phase, the characteristic features of K and of the surface diffusion coefficient (D_s) and their possible relationships should be studied in detail to clarify retention and separation mechanisms in RPLC.

Enthalpy−entropy compensations are a type of extrathermodynamic relationship that is applied to numerous chemical equilibria and kinetic processes to discuss their mechanisms.[9−13] An EEC is demonstrated by a linear correlation between the enthalpy change and the entropy change or, alternatively, by a linear dependence of the enthalpy change on the corresponding free energy change (change associated with the passage of 1 mol of solute from one to the other phase of the system). The slope of the linear plot of the enthalpy change versus the entropy change is called the compensation temperature (T_c), and it is regarded as a process characteristic. Chemical reactions or equilibrium processes that have a similar compensation temperature are considered to be fundamentally related and to have a mechanistic similarity. They are respectively called isokinetic or isoequilibrium processes.[15,24]

Experimental data suggesting EEC for retention equilibria are often reported in RPLC.[14−18] The possibility of such a compensation was also discussed on a theoretical basis.[19−24] Similar values of T_c were obtained under a wide variety of RPLC conditions, e.g., different mobile-phase solvents, sample compounds, and temperature range. It was concluded that the mechanism of interaction of small sample molecules with bonded stationary phases was the same in all RPLC experiments. Although EEC was also found in a normal-phase LC system using a polar stationary phase (Permaphase ETH) and a nonpolar solvent (hexane containing 1% ethanol), the retention mechanism in this system seemed to be different from that in RPLC because the value of T_c was different from that found in RPLC.[15] A compensation behavior was also confirmed for retention equilibria in other systems such as ion-pair RPLC, ion-exchange LC, and gas chromatography. However, very few studies were made for EEC in mass-transfer processes such as surface diffusion.[8,17,25,26]

Analysis of the temperature dependence of either K or the retention factor is the most usual method for estimating the change of enthalpy (ΔH) and entropy (ΔS) associated with the retention equilibrium. However, Krug et al.[19−22] pointed out that linear correlations could well be observed between ΔH and ΔS estimated this way, even when no actual EEC takes place. Such false correlations could arise merely from a compensation between the errors made in the determination of the two parameters of the van't Hoff correlation. These authors showed that the correlation coefficient and the slope of the linear regression due to this statistical compensation effect are close to unity and to the harmonic mean of the experimental temperatures (T_{hm}), respectively. Krug et al.[19−22] suggested four different approaches to determine whether an observed linear correlation between ΔH and ΔS results from an actual physicochemical phenomenon or from the statistical pattern generated by experimental errors. Although many publications discuss the establishment of an EEC for retention equilibria in RPLC, these tests were rarely carried out to discuss in detail the thermodynamic data derived from van't Hoff plots.

Linear free energy relationships constitute another type of extrathermodynamic relationship. The free energy change (ΔG) associated with a chemical equilibrium is linearly correlated with that associated with a related kinetic process or with another reaction equilibrium. Also, ΔG for the equilibrium or the kinetic process is assumed to consist of the sum of incremental contributions due to the various structural elements of the molecule. These empirical correlations of thermodynamic quantities, EEC and LFER, are used to demonstrate the mechanistic similarity of equilibrium or kinetic processes and to study the characteristics of these processes from the viewpoints of molecular structural contributions. Previously, we reported that a LFER is observed between retention equilibrium and surface diffusion in RPLC and

Table 1. Physical Properties of C_{18}-Silica Gel Column and Experimental Conditions

average particle diameter (μm)	45
particle density (g cm^{-3})	0.86
porosity, ϵ_p	0.46
average pore diameter (nm)	14.8
tortuosity factor, k_t[2]	3.6
carbon content (wt %)	17.1
column size (mm)	6 × 150
mass of packing materials (g)	2.1
void fraction	0.42
column temperature (K)	288−308
mobile-phase solvent	methanol/water (70/30, v/v)
superficial velocity (cm s^{-1})	0.06−0.12
sample compounds	*p*-alkylphenols

in other adsorption systems, irrespective of the experimental conditions selected, for instance, of the sample compounds, the nature and composition of the organic modifier in the mobile phase, and the length of alkyl ligands bonded to the stationary phase.[8,17,18,25] However, there are still no sufficient theoretical bases for the derivation of linear correlations between the Gibbs free energies, ΔG, of retention equilibria and of surface diffusion.

In this work, we study the correlation between EECs and LFERs in general but taking as a case in point the properties of RPLC systems using a C_{18}-silica gel and methanol/water mixture (70/30, v/v) as stationary and mobile phases, respectively, and a variety of polar and nonpolar solutes. First, an EEC was found for both retention equilibria and surface diffusion. Second, the four test methods proposed by Krug et al.[19−22] to confirm the validity of an EEC were applied with a positive conclusion. Third, an LFER between the retention equilibrium and surface diffusion was established and discussed. On the basis of the results concerning EEC for retention equilibria and surface diffusion, it was shown that the slope and intercept of this LFER were accounted for by using the compensation temperatures and several other molecular parameters that are related to ΔH and ΔS. The temperature dependence of this LFER was also interpreted.

EXPERIMENTAL SECTION

Column and Reagents. Table 1 lists some physical properties of the C_{18}-silica gel column used (YMC, Kyoto, Japan). This column was packed with relatively large C_{18}-silica gel particles in order to make easier a quantitative analysis of band-broadening phenomena and, more specifically, an accurate estimate of the mass-transfer rate parameters. The mobile phase was a mixture of methanol and water (70/30, v/v). *p*-Alkylphenol derivatives were used as the sample compounds. They were all reagent grade and used without further purification. Sample solutions (concentration, 0.1% w/w) were prepared by dissolving the sample compounds into the mobile phase. Uracil and sodium nitrate were used as inert tracers.

Apparatus. A high-performance liquid chromatograph system (LC-6A, Shimadzu, Kyoto, Japan) was used. Small volumes (2−20 μL) of sample solution were introduced into the mobile-phase stream by using a valve injector (model 7125, Rheodyne, Cotati, CA). A thermostated water bath was used to keep constant the column temperature. The concentration of the sample compounds was monitored with the ultraviolet detector of the HPLC system (SPD-6A).

Procedures. Table 1 lists some of the experimental conditions. Pulse response experiments (i.e., elution chromatography) were carried out at near-zero surface coverage of the sample compounds, in the ranges of column temperature between 288 and 308 K, at volumetric flow rates of the mobile phase that were between 1 and 2 cm^3 min^{-1}. The measurement of the peak retention factors at different flow rates showed these factors to be independent of the flow rate, confirming that the column temperature is radially uniform and that the influence of the pressure on K is negligible (at constant flow rate, the average column pressure changes with the column temperature in inverse proportion to the mobile-phase viscosity).[27] Small concentration pulses or perturbations were introduced into the mobile-phase stream at the column inlet. Other measurements confirmed that a change in the injection volume of sample solution had no influence on the retention factors, suggesting that the pulse response experiments were carried out under linear equilibrium-isotherm conditions. The information regarding the retention equilibrium and the mass-transfer kinetics was derived from the first and the second moment of the elution peaks, respectively, on the basis of the results of the moment analysis method. Details on this method were published previously.[1,4,5,8,17,18] Only some basic information is presented below.

The adsorption equilibrium constant (K) was derived from the first moment (μ_1) of the elution peak:

$$\mu_1 = \frac{\int \mathrm{Ce}(t)t\,\mathrm{d}t}{\int \mathrm{Ce}(t)\,\mathrm{d}t} = \frac{z}{u_0}\left[\epsilon + (1-\epsilon)(\epsilon_p + \rho_p K)\right] \qquad (1)$$

where Ce(t) is the profile of the elution peak, or the concentration of the sample compound in the eluent as a function of t, t the time, z the length of the column, u_0 the superficial velocity of the mobile phase, and ρ_p the particle density. The internal porosity (ϵ_p) of the C_{18}-silica gel particles and the void fraction (ϵ) of the column were derived from the first moment data obtained for uracil and sodium nitrate, both inert tracers.

It has been reported that ionic solutes cannot penetrate into the pore space inside the RP stationary-phase particles because of the Donnan salt exclusion effect when a small amount of electrolyte, such as sodium nitrate, is injected into the column.[28] The elution peak of the electrolyte is then detected at a time corresponding to the extraparticulate void fraction of the column. On the other hand, the elution volume of ionic solutes increases with increasing amount injected into the column if the mobile phase is not buffered. It seems that the electrolyte can completely penetrate into the pores when the amount of electrolyte injected is large enough. The elution volume of ionic solutes should then be equal to the total column void volume. The values of ϵ and ϵ_p were calculated from the elution times of sodium nitrate under these different two injection conditions. The elution volume of uracil should correspond to the total porosity of the column. We confirmed the excellent agreement between the elution volumes of uracil and sodium nitrate when the amount of sodium nitrate injected is sufficiently large.

(27) Szabelski, P.; Cavazzini, A.; Kaczmarski, K.; Liu, X.; Guiochon, G. *J. Chromatogr., A* **2002**, *950*, 41−53.
(28) Wells, M. J. M.; Clark, C. R. *Anal. Chem.* **1981**, *53*, 1341−1345.

The information on the mass-transfer kinetics that is available in the peak profile was derived from the second central moment (μ_2'). As described earlier, it is usually assumed that band broadening results from the mass-transfer resistances due to four different kinetic processes taking place in the column: (1) axial dispersion, (2) fluid-to-particle mass transfer, (3) intraparticle diffusion, and (4) adsorption/desorption at the actual adsorption sites.[1,2,4,5,8] This last contribution to μ_2' was assumed to be negligibly small in RPLC.[7] This moment is related to the column characteristics through the following equation:

$$\mu_2' = \frac{\int \mathrm{Ce}(t)(\mathrm{t} - \mu_1)^2\,\mathrm{d}t}{\int \mathrm{Ce}(t)\,\mathrm{d}t} = \frac{2z}{u_0}(\delta_{ax} + \delta_f + \delta_d) \quad (2)$$

$$\delta_{ax} = (D_L/\mathrm{u_0}^2)\,[\epsilon + (1-\epsilon)(\epsilon_p + \rho_p K)]^2 \quad (3)$$

$$\delta_f = (1-\epsilon)(R_p/3k_f)(\epsilon_p + \rho_p K)^2 \quad (4)$$

$$\delta_d = (1-\epsilon)(R_p^2/15D_e)(\epsilon_p + \rho_p K)^2 \quad (5)$$

where R_p is the radius of the stationary-phase particles and δ is the contribution of each mass-transfer process to μ_2'. The subscripts ax, f, and d denote the axial dispersion, fluid-to-particle mass transfer, and intraparticle diffusion, respectively. Equations 3−5 include three kinetic parameters, the axial dispersion coefficient (D_L), the fluid-to-particle mass-transfer coefficient (k_f), and the intraparticle diffusivity (D_e).

The values of D_e and D_L were derived from μ_2' after subtracting the contribution of fluid-to-particle mass transfer to band spreading. The fluid-to-particle mass-transfer coefficient (k_f) was estimated using the Wilson−Geankoplis equation.[5] The molecular diffusivity (D_m) of the sample compounds in the mobile-phase solvent was calculated by applying the Wilke−Chang equation.[6] Intraparticle diffusion was assumed to consist of two parallel contributions, due to pore and to surface diffusion, respectively,[4,5] with

$$D_e = D_p + \rho_p K D_s \quad (6)$$

where D_p and D_s are the pore diffusivity and the surface diffusion coefficient, respectively. The value of D_s was calculated from the result of the subtraction of the contribution of pore diffusion from the intraparticle diffusivity. The pore diffusivity (D_p) was estimated from D_m, the porosity of the C_{18}-silica gel particles (ϵ_p), the hindrance parameter (K_p), and the tortuosity factor (k_t) of the internal pores.

$$D_p = (\epsilon_p/k_t^2)K_p D_m \quad (7)$$

The value of K_p was calculated with the following equation[29]

$$\log K_p = -2.0\lambda_m \quad (8)$$

where λ_m is the ratio of the diameter of the sample molecule to the average pore diameter. The molecular diameter of the sample compounds was calculated from their molar volume at a normal boiling point on the assumption that the shape of the sample molecules was spherical. The value of K_p does not significantly change in the range between 0.75 and 0.81 for the sample compounds used in this study and uracil. The value of k_t was derived from μ_2' of the uracil peak. The experimental retention time and band dispersion were corrected for the contributions of the extracolumn tubes between the injection valve and the column and between the column and the detector. These contributions were derived from the results of tracer experiments made without a column. The contributions of the moments μ_1 and μ_2' of the sample pulses injected onto the column were ignored because the size of these pulses was extremely small.

Several corrections were made in order to derive D_s from μ_2'. The influence of these corrections on the precision of the conclusions of this study should be considered. As mentioned earlier, the contribution of fluid-to-particle mass transfer to μ_2' was subtracted beforehand during the determination of D_e. An uncertainty in the estimation of k_f affects the results of the second moment analysis. In this study, k_f was derived from the Wilson−Geankoplis equation.[5] For instance, a value $k_f = 3.4 \times 10^{-2}$ cm s^{-1} was obtained for benzene at 298 K when the superficial velocity of the mobile phase is 0.12 cm s^{-1}. A different value, $k_f = 2.6 \times 10^{-2}$ cm s^{-1}, was derived from the equation proposed by Kataoka et al.[5] The corresponding values of D_s were 7.2×10^{-6} and 5.8×10^{-6} cm^2 s^{-1}, respectively. These two values differ by 25%. However, the results of our study are only slightly influenced by variations in the estimated value of k_f because the contribution of the fluid-to-particle mass-transfer resistance to μ_2' is usually no more than 20−30%.[8]

The contribution of D_p to D_e was corrected when D_s was calculated from D_e. As mentioned above, D_p was calculated from D_m, ϵ_p, K_p, and k_t. The accuracy of the estimate of D_m and K_p affects the accuracy of the estimate of D_s. In this study, D_m for the sample molecules in the mobile-phase solvent was calculated using the Wilke−Chang equation.[6] The values of D_m given by this correlation are considered to be in error by less than 10%.[6] The equation proposed by Satterfield et al. (eq 8) was used for estimating K_p. The contribution of surface diffusion to the overall mass transfer in C_{18}-silica gel particles is usually large and as much as nearly 85−95%.[8] Because surface diffusion is the major contribution to intraparticle diffusion in RPLC, the influence of small variations in D_p (hence in D_m and K_p) on the estimate of D_s remains small. The errors made in the estimates of D_m, K_p, and D_p influence little the results of this study. Reasonably accurate results were derived for the retention behavior and the mass-transfer kinetics in the RPLC system studied.

In this study, we propose an LFER model that accounts for the temperature dependence of the slope and the intercept of an LFER with the compensation temperatures, temperatures that are estimated from an EEC analyses. An EEC is conventionally represented as follows.

$$\Delta H = T_c \Delta S + \Delta G_{T_c} \quad (9)$$

where ΔG_{T_c} is the Gibbs free energy change at temperature T_c. Equation 9 implies that, in the vicinity of T_c, changes in ΔH are

(29) Satterfield, C. N.; Colton, C. K.; Pitcher, W. H., Jr. *AIChE J.* **1973**, *19*, 628−635.

offset by changes in ΔS, so that ΔG remains practically independent of the temperature (see eq 10, below).[15] When an actual EEC is established, the Arrhenius or the van't Hoff plots intersect at a point of coordinate $1/T_c$. The value of T_c is derived from the slope of the linear correlation between ΔH and ΔS (see Figure 1a and b). From eq 9 and using the Gibbs−Helmholtz relationship ($\Delta G = \Delta H - T\Delta S$), the free energy change at temperature T is given by

$$\Delta G_T = \Delta H\,(1 - T/T_c) + (T/T_c)\Delta G_{T_c} \qquad (10)$$

In eq 10, a linear correlation should be observed between ΔG_T and ΔH. The slope of the straight line should be equal to $(1 - T_{hm}/T_c)$ when $T = T_{hm}$. The value of T_c can also be calculated from the slope of the linear relationships between ΔG_T and ΔH. In Figure 3a and b (see later), ΔH is plotted against ΔG_{Thm}. In this case, it is obvious from eq 10 that T_c is equal to $T_{hm}/\{1 - 1/(\text{slope})\}$. In this study, T_c was also calculated on the basis of two other equations (see later, eqs 18 and 27). The values of T_c calculated by these different methods are later compared with each other to confirm the validity of the estimates of T_c.

RESULTS AND DISCUSSION

Enthalpy−Entropy Compensation for the Retention Equilibrium and for Surface Diffusion in RPLC. Figure 1a shows a linear correlation between ΔHE and ΔSE. These two thermodynamic functions were respectively estimated from the slope and the intercept of the van't Hoff plot of the logarithm of K versus the reciprocal of the absolute temperature (T),

$$\ln K = -(\Delta H°/RT) + \Delta S°/R \qquad (11)$$

where $\Delta H°$ and $\Delta S°$ are the enthalpy and the entropy changes associated with the retention process, respectively, and R is the gas constant. Similarly, Figure 1b shows a linear correlation between ΔH* and ΔS*, which were estimated from D_s, according to the Arrhenius equation.

$$\ln D_s = -\frac{\Delta H^*}{RT} + \frac{\Delta S^*}{R} + \ln\left(\frac{\lambda^2 k_B T}{h}\right) \qquad (12)$$

where ΔH* and ΔS* are the enthalpy and the entropy of surface diffusion, respectively, λ is the distance between two equilibrium positions, k_B is the Boltzmann constant, and h is the Planck constant. In the absolute rate theory,[30] a diffusion phenomenon is regarded as an activated process of molecular migration from one equilibrium position to another, over the energy barrier between them. λ was estimated as $\sim 3 \times 10^{-8}$ cm from the values of the coefficient D_s for different compounds, values that are of the order of 10^{-6} cm^2 s^{-1} in methanol/water (70/30, v/v) at 298 K.[8] The superscripts ° and * refer to the equilibrium and to the kinetic activation parameters, respectively. The results in Figure 1a and b suggest that EEC is established for both the retention equilibrium and surface diffusion in RPLC. A number of other experimental data suggest EEC for the retention equilibrium in RPLC, with values of $T_c°$ ranging from ~500 to 1000 K.[15,16,18] The slope of the straight line in Figure 1a indicates that $T_c°$ is ~1560 K in this case, a value that is of the same order of magnitude as the previous results. Similarly, a value of T_c* of ~600 K was derived from the parameters of the straight line in Figure 1b. However, there are no data for surface diffusion with which we can compare our result.

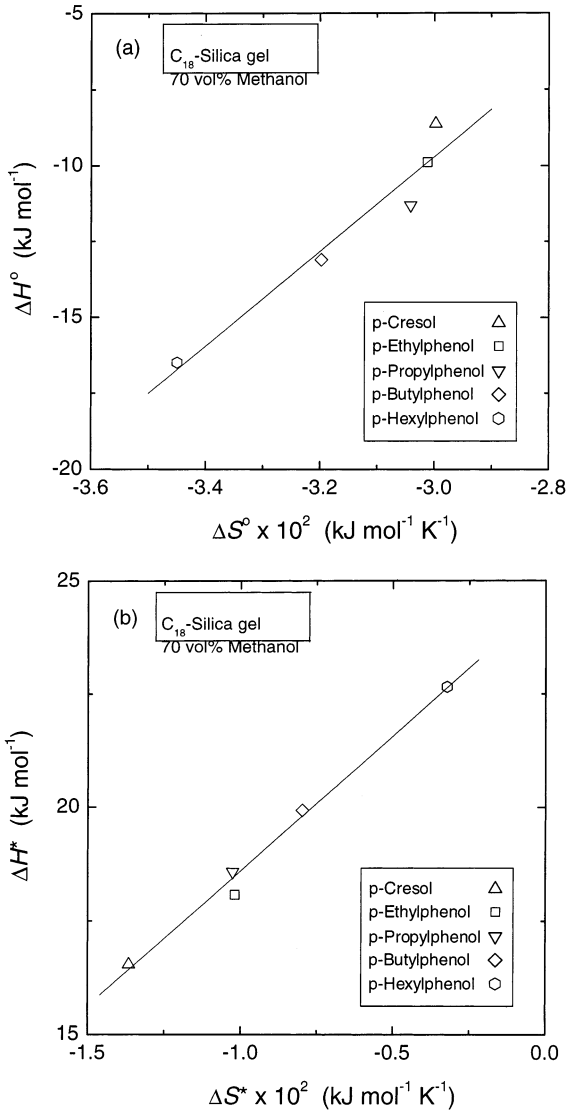

Figure 1. Plot of ΔH vs ΔS for (a) the retention equilibrium and (b) surface diffusion.

In many cases, ΔH and ΔS, whether associated with chemical equilibria or with kinetic processes, are estimated by analyzing the temperature dependence of the equilibrium constants according to the vant Hoff equation or that of the rate coefficients after the Arrhenius equation. However, Krug et al.[19−22] demonstrated that errors are made in the determination of ΔH and ΔS based on linear regressions that distribute these thermodynamic functions along a straight line, the slope and correlation coefficient of which are equal to T_{hm} and close to unity, respectively. Such a correlation may take place even when there is no real EEC effect. These authors proposed four different methods to clarify whether the tentative linear correlation between ΔH and ΔS results from actual physicochemical effects or arises from the statistical

(30) Glasstone, S.; Laidler, K. J.; Eyring, H. *The Theory of Rate Processes*; McGraw-Hill: New York, 1964.

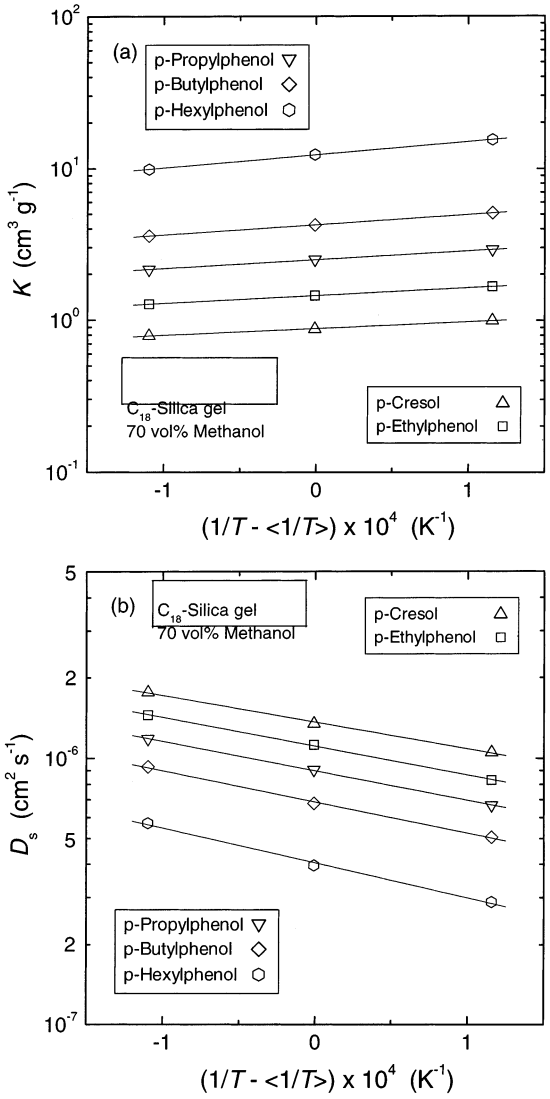

Figure 2. Correlation of (a) K and (b) D_s with $(1/T - \langle 1/T \rangle)$.

compensation due to experimental errors.[19−22] In the following, the experimental data obtained for the retention equilibrium and surface diffusion in the system studied are analyzed on the basis of the four approaches described by Krug et al.

a. Plot of ΔH versus $\Delta G_{T_{hm}}$. If an important physicochemical effect is actually present, the plot of ΔH versus ΔG_{Thm} (i.e., ΔG at T_{hm}) should be linear. Figure 2a shows linear correlations between ln K and $\{1/T - \langle 1/T \rangle\}$. Note that the bracket symbol ($\langle\ \rangle$) indicates an average value, in this case, the arithmetic mean or sum of a series of data divided by the number of data. The values of $\Delta H°$ and $\Delta G°_{T_{hm}}$ for the retention equilibrium were calculated from the slope and intercept of the linear regressions in Figure 2a, respectively

$$\Delta H° = -R(\text{slope}) \tag{13}$$

$$\Delta G°_{T_{hm}} = -RT_{hm}(\text{intercept}) \tag{14}$$

Similarly, Figure 2b shows linear correlations between ln D_s and $\{1/T - \langle 1/T \rangle\}$. The estimates of ΔH^* and $\Delta G^*_{T_{hm}}$ for surface diffusion were calculated as follows.[19−22]

$$\Delta H^* = -R(\text{slope}) - RT_{hm} \tag{15}$$

$$\Delta G_{T_{hm}}{}^* = -RT_{hm}(\text{intercept}) + RT_{hm} \ln\left(\frac{\lambda^2 e k_B T}{h}\right) - RT_{hm} \tag{16}$$

where e is the base of the natural logarithms. Linear correlations are observed between $\Delta H°$ and $\Delta G°_{T_{hm}}$ and between ΔH^* and $\Delta G^*_{T_{hm}}$ in Figure 3a and b, respectively. The compensation temperature for the retention equilibrium ($T_c°$) and surface diffusion (T_c^*) are calculated from the slope of the straight lines in Figure 3a and b as 1680 and 610 K, respectively, according to $T_c = T_{hm}/\{1-1/(\text{slope})\}$.

b. Comparison of T_c with T_{hm} (Hypothesis Test). The values of T_c and T_{hm} should be compared with each other on the basis of the t-test (hypothesis test). The best estimate of T_c should be sufficiently different from T_{hm}. Krug et al.[20] proposed the following equation to test the null hypothesis that T_c was equal to T_{hm}. A minimum and a maximum value of T_c at an approximate $(1 - \alpha_s) \times 100\%$ confidence level were calculated by the following equations.

$$T_c(\text{minimum}) = T_c - t_{m-2,1-\alpha_s}[V(T_c)]^{1/2} \tag{17a}$$

$$T_c(\text{maximum}) = T_c + t_{m-2,1-\alpha_s}[V(T_c)]^{1/2} \tag{17b}$$

with

$$T_c = \frac{\sum(\Delta H - \langle \Delta H \rangle)(\Delta S - \langle \Delta S \rangle)}{\sum(\Delta S - \langle \Delta S \rangle)^2} \tag{18}$$

$$V(T_c) = \frac{\sum(\Delta H - \Delta G_{T_c} - T_c \Delta S)^2}{(m-2)\sum(\Delta S - \langle \Delta S \rangle)^2} \tag{19}$$

where m is the number of (ΔH and ΔS) data pairs and t is the value of the Student t for $m - 2$ data points and a confidence level of $(1 - \alpha_s) \times 100\%$.

Table 2 lists the results of these calculations. The values of $T_c°$ (1560 K) and T_c^* (600 K) calculated by eq 18 are appropriately in agreement with those of T_c obtained for the retention equilibrium and for surface diffusion, respectively. In addition, these values are sufficiently different from T_{hm} (= 298 K). Table 2 also lists the values of T_c(minimum) and T_c(maximum), which are derived from eqs 17a and 17b, for the retention equilibrium and for surface diffusion. According to the t-test, on the basis of these data, the hypothesis of a coincidence of the slope of the $\Delta H - \Delta S$ plot (T_c) with T_{hm} can be rejected at a confidence level of less than 5% for both the retention equilibrium and surface diffusion.

c. Convergence of the van't Hoff and the Arrhenius Plots at Each Corresponding T_c. Panels a and b of Figure 4 show the van't Hoff plots of ln K versus $1/T$ and the Arrhenius plots of ln D_s versus $1/T$, respectively. The linear regression lines intersect, although their intersections do not take place in a single point but in a small region of the plane, due to the influence of experimental errors. In this study, the values of K and D_s were

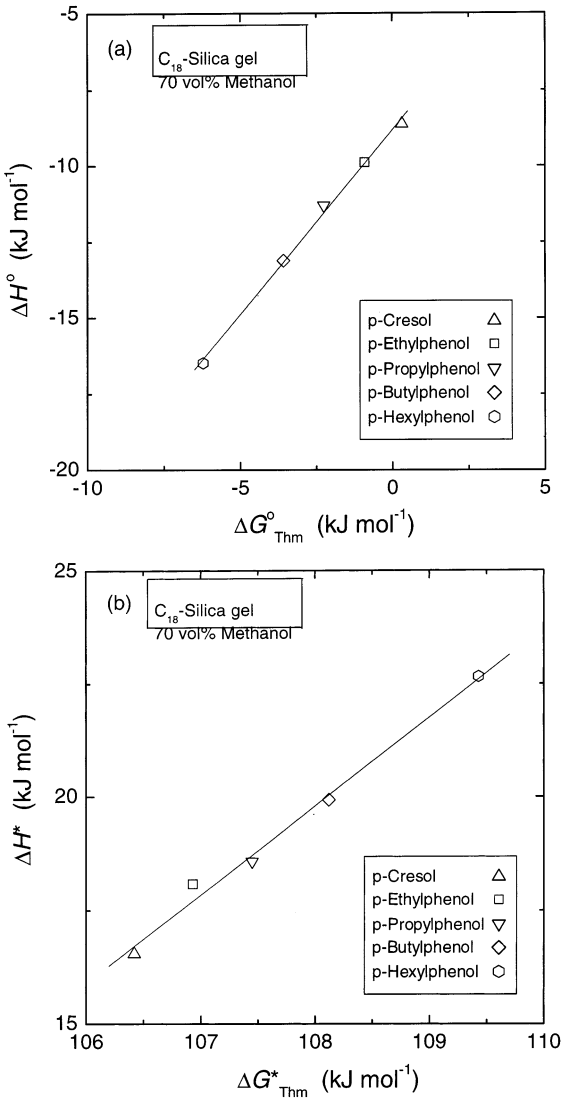

Figure 3. Plot of ΔH vs $\Delta G_{T_{hm}}$ for (a) the retention equilibrium and (b) surface diffusion.

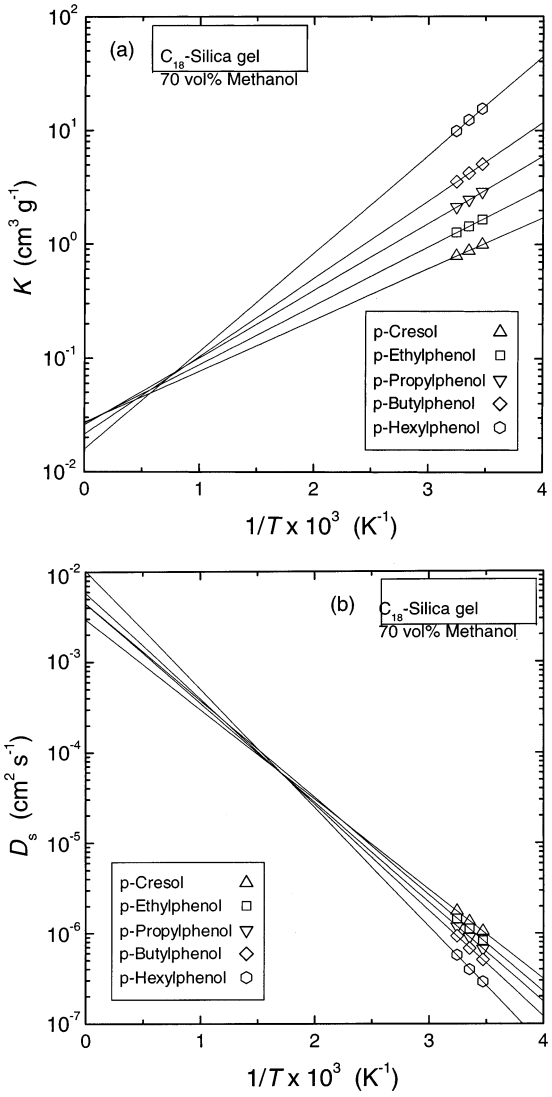

Figure 4. Temperature dependence of (a) K (van't Hoff plot) and (b) D_s (Arrhenius plot).

Table 2. Calculation Results of the Compensation Temperatures

	T_c (K)[a]	T_c (K)[b]	T_c (K)[c] minimum	T_c (K)[c] maximum
retention equilibrium	1680	1560	330	2760
surface diffusion	610	600	400	790

[a] Calculated from the slope of the linear correlations between $\Delta G_{T_{hm}}$ and ΔH. [b] Calculated by eq 18. [c] Range of T_c calculated by eqs 17−19 at the 95% confidence level.

measured at three different temperatures (288−308 K), a rather narrow range compared with the difference between the intersection points and the experimental temperatures. This may explain the distribution of the intersection points. The compensation temperatures estimated from the intersection points in Figure 4a and b are fairly close to the values of $T_c°$ and T_c* obtained as described above.

d. Probability for the Intersection of the van't Hoff and Arrhenius Plots. According to the *F*-test, the probability for the intersection of the linear regression lines should be compared with that for a nonintersection, on the basis of the statistical data derived by an analysis of variance (ANOVA) procedure.[22] The probability for nonintersection should also be compared to the precision of the experimental data in the same manner.

Table 3 lists the values of the mean sum of squares calculated. For the retention equilibrium, the mean sum of squares of the intersection (MS_{con}) is ~3 orders of magnitude larger than that of the nonintersection (MS_{noncon}). The ratio MS_{con}/MS_{noncon} is ~60 times larger than the *F*-value, $F(1, 3, 1 - \alpha_s = 0.975) = 17.4$, indicating that the probability for the intersection is sufficiently high compared with that for nonintersection. Similarly, the ratio of MS_{noncon} to the mean sum of squares of the residuals (MS_ϵ) was sufficiently smaller than the corresponding *F*-value, $F(3, 4, 1 - \alpha_s = 0.975) = 9.98$. The negative value of MS_ϵ seems to result from calculation errors and suggests that the variation due to the errors of measurement is quite small. The probability for nonconcurrence is found to be smaller than the precision of the experimental data.

The same conclusion is obtained for surface diffusion. MS_{con} is ~80 times larger than MS_{noncon}. The ratio MS_{con}/MS_{noncon} is ~5

Table 3. ANOVA Table for the Retention Equilibrium and Surface Diffusion in RPLC

source of variation	DF[a]	retention equilibrium SS[b]	retention equilibrium MS[c]	surface diffusion SS[b]	surface diffusion MS[c]
total	14	1.3×10^{1}	9.1×10^{-1}	3.6	2.6×10^{-1}
rows (samples)	4	1.2×10^{1}	3.1	2.6	6.6×10^{-1}
columns (temperatures)	2	2.6×10^{-1}	1.3×10^{-1}	8.0×10^{-1}	4.0×10^{-1}
interactions	8	1.3×10^{-2}	1.6×10^{-3}	2.1×10^{-1}	2.6×10^{-2}
slope	4	1.4×10^{-2}	3.5×10^{-3}	8.2×10^{-3}	2.0×10^{-3}
concurrence	1	1.4×10^{-2}	1.4×10^{-2}	7.9×10^{-3}	7.9×10^{-3}
nonconcurrence	3	4.0×10^{-5}	1.3×10^{-5}	3.0×10^{-4}	9.9×10^{-5}
residuals	4	-7.3×10^{-4}	-1.8×10^{-4}	2.0×10^{-1}	5.1×10^{-2}

[a] Degree of freedom. [b] Sum of squares. [c] Mean sum of squares.

times larger than the F-value, $F(1, 3, 1 - \alpha_s = 0.975) = 17.4$. The probability of concurrence is greater than that of nonconcurrence at the $100\alpha_s$% level of significance. On the other hand, the ratio of MS_{noncon} is ~500 times smaller than MS_ϵ. The ratio MS_{noncon}/MS_ϵ is ~5000-fold smaller than the corresponding F-value, $F(3, 4, 1 - \alpha_s = 0.975) = 9.98$. The variation due to nonconcurrence is not greater than that due to the measurement errors at the $100\alpha_s$% level of significance.

On the basis of all the results described in this section, we may conclude that the linear correlation in Figure 1a accounts for the real EEC for the retention equilibrium originating from actual physicochemical effects taking place in the RPLC system. Similarly, the linear correlation in Figure 1b demonstrates that an actual EEC is also established for the kinetic process, surface diffusion, in the RPLC system studied here. In previous papers,[8,17,25,26] we reported the EEC correlations for the retention equilibrium and surface diffusion in RPLC. In this study, we discussed the establishment of the EEC in more detail on the basis of the four approaches proposed by Krug et al.

Linear Free Energy Relationship between the Retention Equilibrium and Surface Diffusion in RPLC. Because adsorbate molecules migrate by surface diffusion in the adsorbed state, the presence of some sort of correlation is expected between K and D_s. Figure 5 shows that $\ln D_s$ is linearly correlated with $\ln K$, suggesting that an LFER is found in the RPLC system.[8]

$$\ln D_s = A \ln K + B \tag{20}$$

where A and B are the slope and intercept of the straight line, respectively. Although the linear correlations in Figure 5 are almost parallel, the values of A and B depend to some extent on the experimental conditions of RPLC. The parameter A contains information on the correlation between the activation energy of surface diffusion and the adsorption enthalpy. On the basis of the results in Figure 1, eqs 11 and 12 suggest that the slope of the linear correlations in Figure 5 is almost equal to the ratio of ΔH^* to ΔH°. It is probably necessary for an adsorbed molecule to gain an activation energy for breaking the adsorptive interaction between the adsorbate molecule and the surface of the stationary phase when the molecule migrates by surface diffusion. Because $|A|$ is ~0.5, the activation energy ($\Delta H^* + RT$) should be smaller than $-\Delta H^\circ$ and approximately equal to half $-\Delta H^\circ$. On the basis of this consideration, we derived a surface-restricted molecular diffusion model as a first approximation for the mass-transfer

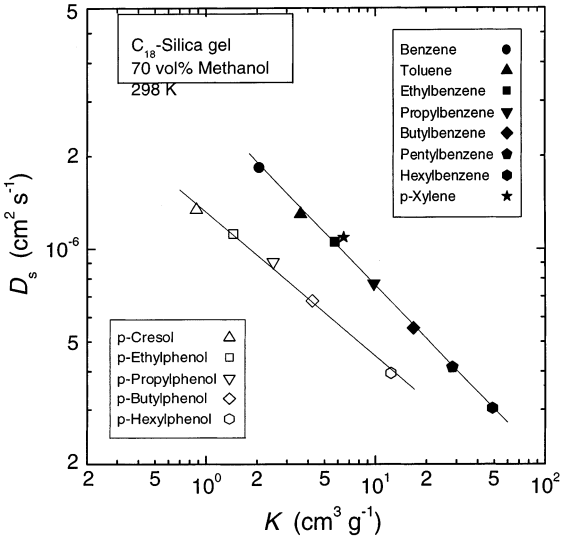

Figure 5. Correlation between D_s and K.

mechanism of surface diffusion.[8,17,18,25] In the following, the physical meaning and the temperature dependence of the parameters A and B are discussed in more detail.

The free energy changes for the retention equilibrium (ΔG°) and surface diffusion (ΔG^*) are written with K and D_s, respectively, as follows:

$$\Delta G^\circ = -RT \ln K \tag{21}$$

$$\Delta G^* = -RT \ln K^* = -RT \ln (D_s h/\lambda^2 k_B T) \tag{22}$$

where K^* is the hypothetical equilibrium constant between the steady state and the transition state.[30] Note that the ratio in the parentheses of the right-hand side in eq 22 is represented as $kh/(k_B T)$ when eq 22 is written for first-order rate constants (k) instead of D_s.[30] The two free energy changes, ΔG° and ΔG^*, are linearly correlated with each other as described by the following equation derived from eqs 20 to 22.

$$\Delta G^\circ = \alpha \Delta G^\circ + \beta = A \Delta G^\circ - RTB - RT \ln (h/\lambda^2 k_B T) \tag{23}$$

Many authors have discussed the conditions necessary for the existence of LFERs.[9–13] However, some of LFER's characteristics, e.g., the temperature dependence of their parameters, are not elucidated yet. Although it is well known that the existence of an

LFER rests on that of an EEC, there are no close quantitative relationships between LFER and EEC either.[12,13]

On the other hand, the following equation was proposed to correlate ΔG of a molecule involved in hydrophobic interactions with a certain molecular property, X_m.[24,31]

$$\Delta G = a_g X_m + b_g \quad (24)$$

where a_g is increment of ΔG per unit value of the molecular property X_m and b_g is ΔG at $X_m = 0$. Various molecular properties can be taken for X_m, for instance, the nonpolar surface area of the molecule or the number of reccurring structural elements, e.g., the methylene group. Similar representation may be written for the enthalpy and entropy changes.[24,31]

$$\Delta H = a_h X_m + b_h \quad (25)$$

$$\Delta S = a_s X_m + b_s \quad (26)$$

The number of methylene groups (N_m) in the sample molecules can be taken for X_m. It was experimentally demonstrated that ΔG and ΔH are accounted for by linear functions of N_m in the sample molecules.[3,8,14,32] As a consequence, linear correlations would be predicted between ΔS and N_m for both the retention equilibrium and surface diffusion. Figure 6 shows plots of $\Delta H°$, $\Delta S°$, $\Delta H*$, and $\Delta S*$ derived from the linear correlations in Figure 2 as functions of N_m. Linear correlations observed between the four thermodynamic parameters and N_m suggest the validity of eqs 25 and 26. Table 4 lists the values of the slope a and intercept b for the sample series of *p*-alkylphenols. With the molecular parameters a and b, T_c can be expressed as[24]

$$T_c = a_h / a_s \quad (27)$$

According to eq 27, we could calculate that $T_c°$ and T_c* are respectively equal to 1680 ($= -1.59/(-9.46 \times 10^{-4})$) and 610 K ($= 1.19/(1.95 \times 10^{-3})$), values that are in agreement with the values of $T_c°$ (1680 K) and T_c* (610 K) obtained as described above.

Differentiating both sides of eq 23 with respect to N_m gives,

$$\partial \Delta G* / \partial N_m = A \partial \Delta G° / \partial N_m \quad (28)$$

The following equation is derived from eqs 25 and 26, according to the Gibbs−Helmholtz relationship

$$\Delta G = \Delta H - T\Delta S = (a_h N_m + b_h) - T(a_s N_m + b_s) \quad (29)$$

Substituting eq 29 into eq 28 and rearranging gives,

$$\alpha = A = a_s*(T_c* - T)/a_s°(T_c° - T) \quad (30)$$

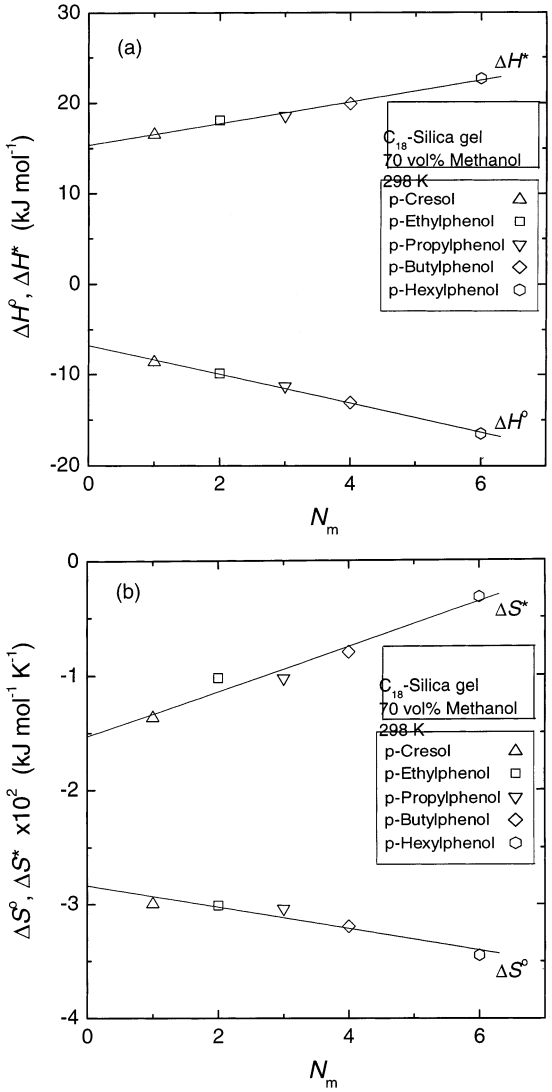

Figure 6. Correlation of (a) ΔH and (b) ΔS with N_m.

Table 4. Molecular Thermodynamic Parameters for *p*-Alkylphenols

	slope		intercept	
$\Delta H°$ vs N_m	−1.6	($a_h°$)	−6.8	($b_h°$)
$\Delta S°$ vs N_m	-9.5×10^{-4}	($a_s°$)	-2.8×10^{-2}	($b_s°$)
$\Delta H*$ vs N_m	1.2	(a_h*)	1.5×10^{1}	(b_h*)
$\Delta S*$ vs N_m	2.0×10^{-3}	(a_s*)	-1.5×10^{-2}	(b_s*)

where $a_s°$ and a_s* are the variation of ΔS corresponding to a unit increment of the number of methylene groups for the retention equilibrium and surface diffusion, respectively. Equation 30 indicates that α (A) depends on the temperature and is correlated with $T_c°$ and T_c*. On the other hand, by substituting eq 30 into eq 23, β (B) is given by

$$\beta = -RTB - RT \ln (h/\lambda^2 k_B T) = [(b_h* - Tb_s*) - \alpha(b_h° - Tb_s°)] \quad (31)$$

Figure 7 shows the complex temperature dependence of A and B. With increasing temperature, A increases but is discontinuous at $T = T_c°$. In addition, A is equal to zero at $T = T_c*$. The slope of the curve for A depends on T. A similar profile is observed for

(31) Lee, B. *Proc. Natl. Acad. Sci. U.S.A.* **1991**, *88*, 5154−5158.
(32) Krstulović, A. M.; Brown, P. R. *Reversed-Phase High-Performance Liquid Chromatography*; John Wiley & Sons: New York, 1982.

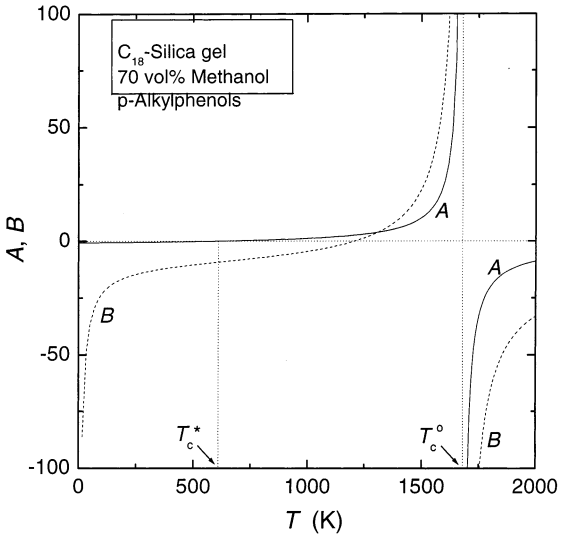

Figure 7. *A* and *B* as a function of *T*.

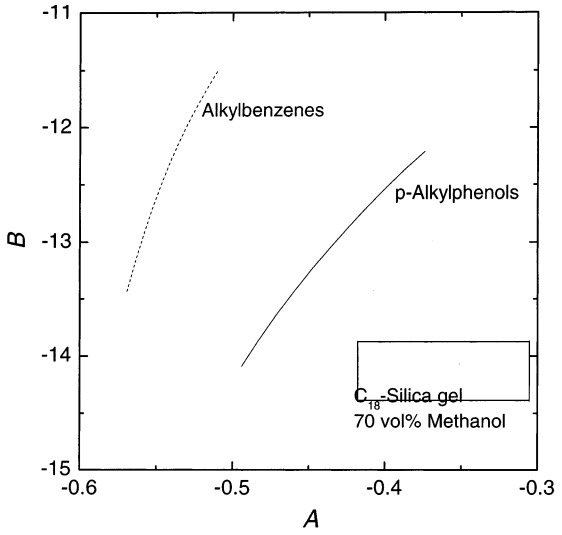

Figure 8. Plot of *A* vs *B*.

B. Because of the similarity of the profiles for *A* and *B*, it is expected that a simple correlation would be obtained between *A* and *B* in a narrow temperature range. Figure 8 shows slightly curved correlations between *A* and *B* for the *p*-alkylphenols and alkylbenzenes around room temperature at which the chromatographic experiments were made in this study. Although the two correlations in Figure 8 show a similar trend, they are not in total agreement with each other. Because *A* and *B* are accounted for by thermodynamic parameters depending on the structural and physicochemical properties of the sample molecules, the difference in the correlations observed between ln D_s and ln *K* in Figure 5 results from the characteristics and mechanisms of the molecular interactions between the sample compounds and the surface of the stationary phase.

Figure 9 shows the temperature dependence of the correlation between ln D_s and ln *K* for the *p*-alkylphenol homologues. The symbols represent the experimental data between 288 and 308 K and the values calculated at $T = T_c^* = 610$ K and $T = T_c^\circ = 1680$ K. Figure 10 shows enlargements of the experimental plots in Figure 9. The solid and dotted lines are drawn based on the experimental data and the correlation between *A* and *B* in Figure

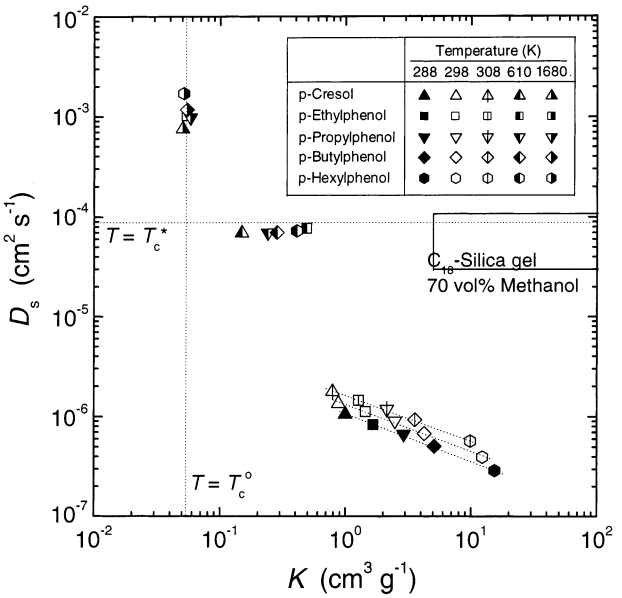

Figure 9. Temperature dependence of the correlation between D_s and *K*.

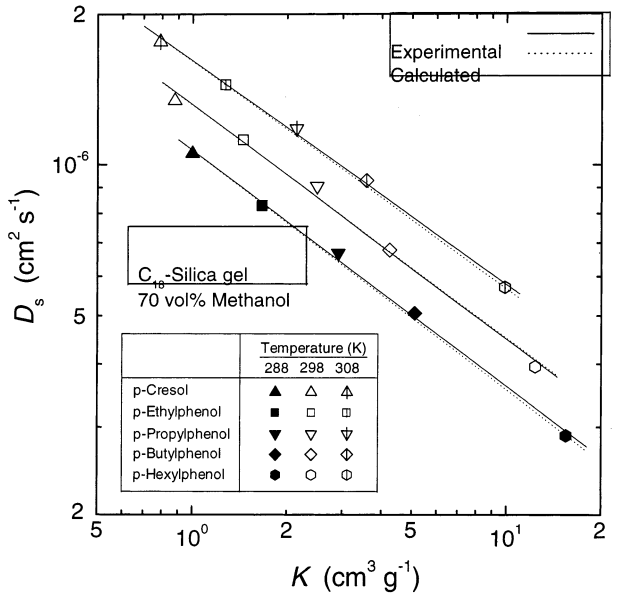

Figure 10. Enlargement of the plot of the experimental data in Figure 9.

8, respectively. The dotted lines agree well with the experimental plots and the solid lines, indicating that the characteristic features (slope and intercept) and the temperature dependence of the linear correlation between ln D_s and ln *K* are properly interpreted by eqs 30 and 31. These equations are based on the conclusive results of two correlations for both the equilibrium and the kinetic processes in RPLC. The first correlation is the EEC between ΔH and ΔS, and the other is the Martin correlation between thermodynamic parameters and chemical structure of the adsorbate molecules. The agreement between the experimental data and the calculated lines proves the validity and consistency of the simple model of LFER derived here.

Figure 9 also shows hypothetical correlations between ln D_s and ln *K* at $T = T_c^*$ and $T = T_c^\circ$. The corresponding plots were calculated from the vant Hoff equation and the Arrhenius equation,

deduced from the retention and surface diffusion data in the temperature range $288 < T < 308$ K because it was impossible to measure experimental data at higher temperatures. The horizontal and vertical linear lines show the values expected at $T = T_c^*$ and $T = T_c^\circ$. The calculated plots scatter around the lines. Although RPLC separations cannot be carried out at the high temperatures indicated, it is important that the dependence of LFER on temperature is well accounted for by eqs 30 and 31. The results in Figure 9 show that eqs 30 and 31 allow the prediction of the temperature dependence of an LFER.

CONCLUSION

We demonstrated that EEC was found for both the retention equilibrium and surface diffusion in a simple RPLC system. Linear correlations were observed between ΔH and ΔS estimated from the temperature dependence of K, by applying the van't Hoff equation, and from that of D_s, by using Arrhenius equation. An analysis of the experimental retention and surface diffusion data according to the four methods proposed by Krug et al. indicates that the linear correlations observed between ΔH° and ΔS° and between ΔH^* and ΔS^* originate from an actual EEC based on substantial physicochemical effects and gave values of T_c° and T_c^* equal to 1680 and 610 K, respectively, for *p*-alkylphenol homologues.

We also demonstrated that ΔH and ΔS for both the retention equilibrium and surface diffusion in RPLC were all linearly correlated with the number N_m of methylene groups. The slope (a) and intercept (b) of the linear correlations between ΔH or ΔS and N_m are related to different extrathermodynamic properties such as T_c and ΔG_{Tc}. For instance, the ratios a_h°/a_s° and a_h^*/a_s^* were close to the respective compensation temperatures, T_c° and T_c^*, respectively. The slope (A) and intercept (B) of the LFER between ln K and ln D_s are accounted for by the compensation temperatures (T_c° and T_c^*) and the molecular thermodynamic parameters (a and b). A molecular interpretation was provided for the physical meanings of A and B by assuming that ΔH or ΔS are the sums of enthalpy or entropy increments contributed by the structural elements. Ultimately, the characteristics of EEC and LFER (T_c°, T_c^*, α, A, β, B) depend on structural parameters (a and b).

The influence of the temperature on LFER was clarified. A is equal to zero at $T = T_c^*$. A and B are functions of T and are discontinuous at $T = T_c^\circ$. In the case under study, the intimate correlations between EEC and LFER and the temperature dependence of the LFER were quantitatively interpreted in connection with some molecular parameters.

Although we discussed here the quantitative interpretation of the relation between EEC and LFER in the case of retention equilibrium and surface diffusion in RPLC, the conclusions of this work and the equations derived are by no means limited to RPLC systems. The validity of the simple model presented should be extended to many other chemical reaction systems. The analysis of numerous sets of reliable experimental data is in progress.

GLOSSARY

a	slope of the linear correlation between a thermodynamic property and X_m
A	slope of LFER
b	intercept of the linear correlation between a thermodynamic property and X_m
B	intercept of LFER
D_e	intraparticle diffusivity (cm^2 s^{-1})
D_L	axial dispersion coefficient (cm^2 s^{-1})
D_m	molecular diffusivity (cm^2 s^{-1})
D_p	pore diffusivity (cm^2 s^{-1})
D_s	surface diffusion coefficient (cm^2 s^{-1})
ΔG	free energy change (kJ mol^{-1})
h	Planck constant (J s)
ΔH	enthalpy change (kJ mol^{-1})
k	first-order rate constants (s^{-1})
k_B	Boltzmann constant (J K^{-1})
k_f	fluid-to-particle mass-transfer coefficient (cm s^{-1})
k_t	tortuosity factor
K	adsorption equilibrium constant (cm^3 g^{-1})
K_p	hindrance parameter
m	number of (ΔH and ΔS) data pairs
MS	mean sum of squares
N_m	number of methylene groups
R	gas constant (J mol^{-1} K^{-1})
R_p	particle radius (μm)
ΔS	entropy change (J mol^{-1} K^{-1})
T	absolute temperature (K)
T_c	compensation temperature (K)
T_{hm}	harmonic mean of experimental temperatures (K)
t	time (s)
u_0	superficial velocity (cm s^{-1})
X_m	property of molecule
z	column length (cm)

Greek Symbols

α	slope of LFER
α_s	statistical level of significance
β	intercept of LFER
δ	contribution of mass-transfer resistance to μ_2' (s)
ϵ	void fraction (external) porosity of the column
ϵ_p	porosity of the stationary-phase particle
λ	distance between two equilibrium positions (cm)
λ_m	ratio of the diameter of sample molecule to the average pore diameter
μ_1	first moment (s)
μ_2'	second central moment (s^2)
ρ_p	particle density (g cm^{-3})

Superscripts

$^\circ$	referring to equilibrium parameters
*	referring to kinetic activation parameters

Subscripts

ax	axial dispersion
con	concurrence

d	intraparticle diffusion
f	fluid-to-particle mass transfer
g	free energy change
h	enthalpy change
noncon	nonconcurrence
s	entropy change
T_c	at compensation temperature
T_{hm}	at harmonic mean of experimental temperatures
e	referring to measurement errors

ACKNOWLEDGMENT

This work was supported in part by a Grant-in-Aids for Scientific Research (12640581) from the Japanese Ministry of Education, Science and Culture, by Grant CHE-00-70548 from the National Science Foundation, and by the cooperative agreement between the University of Tennessee and the Oak Ridge National Laboratory.

Received for review April 15, 2002. Accepted August 26, 2002.

AC020245P